TOMOGRAPHIC IMAGING OF AN ULTRASONIC FIELD IN A PLANE USING A LINEAR ARRAY

Patrick H. Johnston[1] and Kendall R. Waters[2†]

[1]NASA Langley Research Center, Hampton, VA 23681
[2]Department of Physics, Washington University, St. Louis, MO 63130

ABSTRACT. A method is presented based on tomographic reconstruction techniques for the visualization of an ultrasonic field. The tall, narrow piezoelectric elements of a one-dimensional receiving array, rotated about its central axis, provide parallel projection input data for tomographic reconstruction of the field. The technique is demonstrated using simulated ultrasonic beams and experimental measurements of an ultrasonic beam propagated through a stitched woven composite.

INTRODUCTION

Research is producing increasingly complex materials for use in aerospace and other applications. These advanced material architectures include such developments as multidimensional fiber-reinforced plastics incorporating textiles and stitching [1], materials with embedded sensors and actuators [2], and other multifunctional materials concepts. A feature common to all of these "smart materials" is that they exhibit increased spatial variability of material properties, requiring an increased number of parameters to describe their state. These spatial variations occur on a scale significant to ultrasonic waves at the frequencies used for NDE. Because of this information-rich propagation environment, an interrogating ultrasonic field becomes phase-distorted as it gathers material information along its path. Conventional single-element ultrasonic sensors phase-sensitively average the received ultrasonic field. The phase-distortions within the field thus manifest themselves as a kind of coherent "noise" on the received signal. A conclusion can be reached that *increasingly complex materials require increasingly sophisticated NDE.*
Multiple-element ultrasonic arrays can be used as a means to provide additional degrees of measurement freedom. By exploiting the additional degrees of freedom, it may be possible to measure and interpret the distorted ultrasonic field emerging from a complex material, effectively converting the "noise" into "signal" for more complete quantitative NDE of the material. Within the context of exploiting these additional degrees of freedom, the concept was identified of *using a rotated linear array receiver to perform tomographic reconstruction of an ultrasonic beam*.

† Present affiliation NIST, Boulder, CO

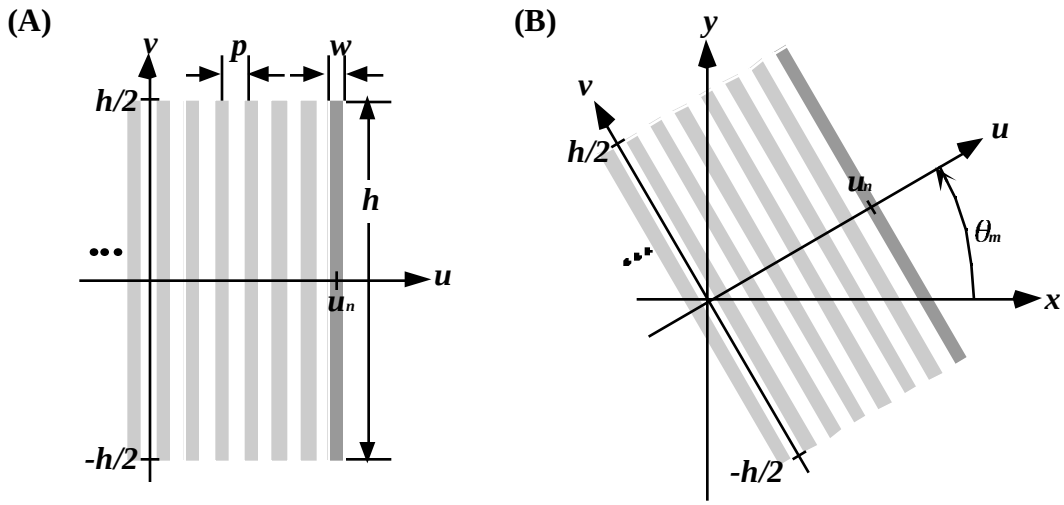

FIGURE 1. (A) Geometry of a linear ultrasonic array. Each element face has area $w \times h$ and the elements are spaced by p. (B) Geometry of rotated linear array.

CONCEPT

Consider the linear array depicted in Fig. 1A. The elements of the linear array have height h and width w, with center-to-center spacing p. The ultrasonic field incident on the array has magnitude and phase characteristics, and can be expressed in the form

$$p(u, v, t) = P(u, v)\ e^{i\psi(u,v) - i\omega t} = \left[p_R(u, v) + i\ p_I(u, v) \right] e^{-i\omega t}. \qquad (1)$$

Here, the complex spatial variation has been separated into real and imaginary parts. The voltage $V(u_n, t)$ produced by the n^{th} element, centered at u_n, is proportional to the integral of the pressure over the active area of the element,

$$V(u_n, t) \propto e^{-i\omega t} \int_{u_n - w/2}^{u_n + w/2} \int_{-h/2}^{h/2} \left[p_R(u, v) + i\ p_I(u, v) \right] dv\ du. \qquad (2)$$

If the pressure variation in the u direction over a distance w is small, the u integral can be performed trivially, yielding a line integral of pressure over v,

$$V(u_n, t) \propto e^{-i\omega t}\ w \int_{-h/2}^{h/2} \left[p_R(u_n, v) + i\ p_I(u_n, v) \right] dv\ . \qquad (3)$$

This can be viewed as a *projection integral* of the pressure along v at the horizontal location u_n. The physical array elements are parallel and evenly spaced along u, and thus produce a set of voltages which represent *parallel projection integrals* of the incident pressure.

If the field is now considered to be fixed in a reference frame (x, y) and the linear array lies in a reference frame (u, v) rotated by angle θ_m relative to (x, y), as depicted in Fig. 1B, the coordinate frames are related according to

$$u(\theta_m) = x \cos(\theta_m) + y \sin(\theta_m),\ v(\theta_m) = -x \sin(\theta_m) + y \cos(\theta_m)\ . \qquad (4)$$

The set of voltages $\{V(u_n(\theta_m), t);\ n = 1, 2, \ldots, N;\ m = 1, 2, \ldots, M\}$, acquired at each of the N array elements at each of M angles, equally distributed between 0 and π, represent a complete set of data input for *tomographic reconstruction by filtered backprojection of parallel projection data*[‡]. The filtered backprojection algorithm can thus be applied to $\{V(u_n(\theta_m),t)\}$ in order to reconstruct the pressure field $[p_R(x, y) + i\, p_I(x, y)]$.

TOMOGRAPHIC RECONSTRUCTION – SIMULATION

Simulated Ultrasonic Beam in Water

Simulated ultrasonic beams were computed using the angular spectrum decomposition technique [3]. Fig. 2 shows the imaginary part of a simulated 2.25 MHz ultrasonic beam produced in water by a 12.7 mm diameter, 50 mm focal length circular transducer, at a distance of 50 mm. Superimposed on the image are the outlines of the elements of a simulated linear array transducer. (For the sake of visualization, the figure contains only 32 elements which are twice the width of the actually simulated ones.) The field was calculated over a 25.6 mm square area, at a pixel resolution of 0.1 mm (256 x 256 pixels). The 64 simulated array elements were 10.00 mm (100 pixels) tall by 0.20 mm (2 pixels) wide, with a gap of 0.10 mm (1 pixel) between elements. The signal from each element was computed by summing all the pixels within the element. The process was repeated for the real and imaginary parts of the simulated beam. Because of symmetry, the resulting set of data for all rotation angles would be identical, so the data were reproduced to simulate measurement at 64 angles, spaced by 5.625° increments. Filtered backprojection was performed to reconstruct the real and imaginary parts of the simulated beam. From the real and imaginary parts, the magnitude and phase were computed, and a two-dimensional phase unwrapping algorithm was applied.

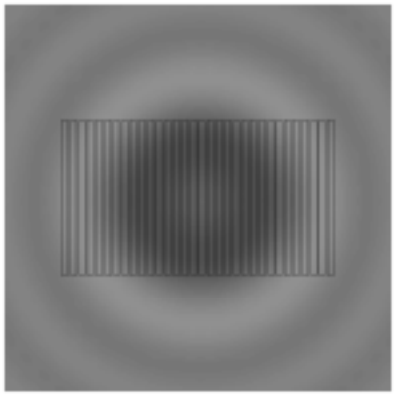

FIGURE 2. Imaginary part of a simulated ultrasonic beam in water, with the outlines of the elements of a receiving linear array superposed. For visualization purposes, this figure depicts half the actually simulated number of elements at twice the actually simulated width.

[‡] The filtered backprojection algorithm is also known as the Radon transform. Some commercial math packages include an implementation of the Radon transform [4,5]. A comprehensive development of the technique is given by Kak [6].

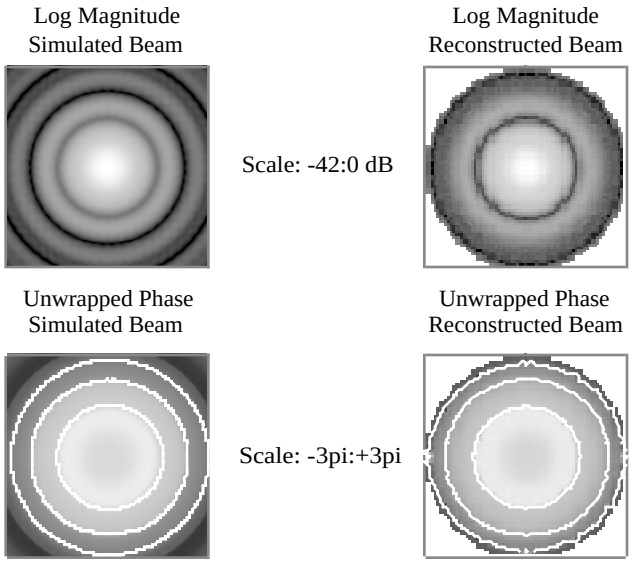

FIGURE 3. Comparison of the log magnitude and phase of the original simulated beam data (left) and the reconstructed log magnitude and phase (right). Phase images have contours at multiples of π.

Reconstructed Field

The log magnitude and the unwrapped phase [7] of the simulated ultrasonic beam is presented on the left-hand panels of Fig. 3. On the right-hand side are the log magnitude and unwrapped phase of the reconstructed ultrasonic beam. The field is not reconstructed beyond the area swept out by the rotating array. The reconstructed data match very well with the original field.

TOMOGRAPHIC RECONSTRUCTION – EXPERIMENT

Data acquisition

The data acquisition configuration is presented in Fig. 4. In a water tank, a 64-element linear array (2.25 MHz, 10 mm by 19.2 mm area) was mounted vertically on a turntable, centered on the axis of rotation. Coaxial with the array, a single-element circular transmitting transducer (2.25 MHz, 12.7 mm diameter, 50 mm focal length) was mounted.

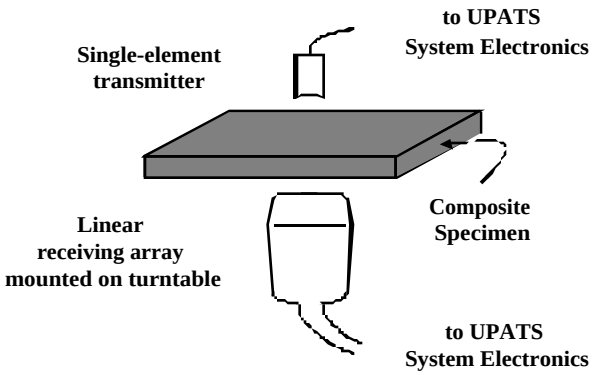

FIGURE 4. Data acquisition setup. A single-element circular focused transmitting transducer is mounted coaxially with a 64-element linear receiving array, which is mounted centered on a turntable, allowing rotation through a full 360°. A specimen can be inserted between the transducers.

The two were separated by 55 mm to allow the placement of a specimen at the focal distance of the transmitting transducer. The transmitting transducer and the receiving array were connected to the NASA Langley Ultrasonic Phased Array Testbed System (UPATS). The transmitter was driven by a 10-cycle tone burst at 2.25 MHz. The signal received by each of the 64 array elements was digitized (50 MHz sampling rate, 1024 points) and a discrete Fourier transform was performed to extract the real and imaginary parts at 2.25 MHz. The measurement was repeated for each of 64 rotational positions of the turntable separated by 5.625°.

This measurement procedure was followed first with only water between the transducers. Subsequently, a stitched composite specimen was positioned between the transducers, and the measurement procedure was repeated at each of two locations on the specimen, to be described below.

Stitched composite specimen

Fig. 5A is a cross-sectional sketch of the fiber architecture in a stitched fiber-reinforced composite material. The composite is built up of layers of fibers, depicted here as straight, but may be mats of woven, braided, or knitted fiber bundles. The layers are held together by a sewing stitch, which consists of a doubled length of fibers penetrating through the thickness of the composite. Under a typical standard ultrasonic inspection, an ultrasonic beam would be incident perpendicular to the surface of the part. The stitch fibers present a locally increased stiffness, and hence wave speed, which results in wavefront distortion, and the stitch fibers also provide additional scattering and other loss mechanisms.

In Fig. 5B is a transmission C-scan of a stitched composite material, 10 cm on each side. The textile layers are woven carbon fibers, the stitch material is Kevlar, and the matrix is epoxy. At the locations of the through-thickness stitches, the signal loss is greatest, producing dark spots in the image. Also, the woven fabric produces variations in the background image. For this study, an ultrasonic beam was propagated through a composite location between stitches, where the woven textile architecture alone was interrogated, and through a location directly over a stitch. As a dimensional reference, the outline of a reconstructed beam area is illustrated by a broken square in Fig. 5B.

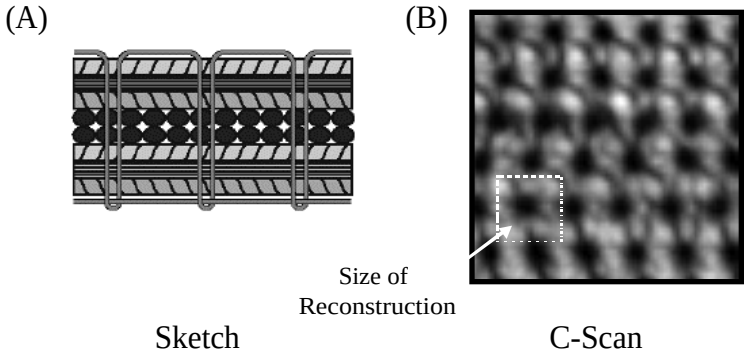

FIGURE 5. (A) Sketch of the cross-section of a stitched, laminated fiber-reinforced composite. (B) Ultrasonic C-scan of a stitched woven composite. Higher attenuation (dark spots) occur where the stitches penetrate the thickness of the panel. The fiber waviness in the woven fabric results in variation of the ultrasonic signal between the stitches. The size of tomographic reconstruction is indicated by a broken line.

Ultrasonic Beam Through Water Path

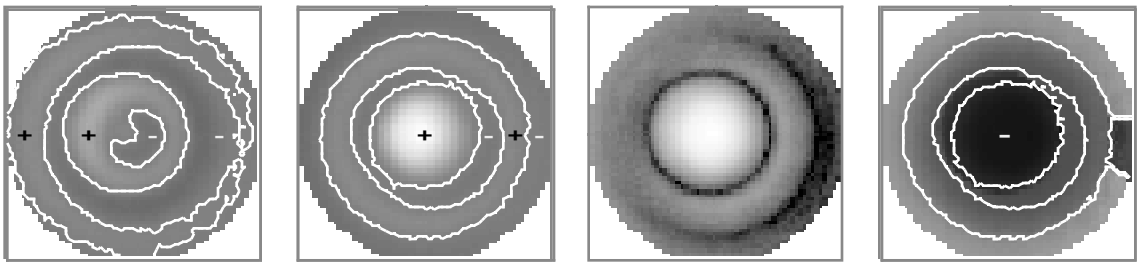

Real Part | Imaginary Part | Log Magnitude | Unwrapped Phase

FIGURE 6. Reconstructed beam through water path. Reconstructed real and imaginary parts have zero-crossing contours to indicate sign change. The log magnitude data is scaled from –42 dB to 0 dB. Unwrapped phase has contours at multiples of π.

RESULTS

Reconstructed beam through water

Fig. 6 presents the reconstructed field derived from data taken through a water-only path. From left to right, the images are of the real part and the imaginary part of the pressure, followed by the log magnitude and the unwrapped phase derived from the first two quantities. The real and imaginary part data have both positive and negative values. Contours are superposed to indicate the zero crossings, and + and – symbols indicate the sense of the data between the contours. Unwrapped phase has contours at multiples of π. In this, as in subsequent images of unwrapped phase, there are some phase artifacts around the outer portion of the image, where the signal-to-noise ratio is smaller.

While there is evidence in these results of an angular misalignment between the transmitting transducer and the plane of the linear array, the error is small and the circular symmetry of the beam is predominantly preserved.

Reconstructed beam through woven composite

In Fig. 7 are presented the reconstructed images for a beam transmitted through a woven composite between the through-the-thickness stitches. As before, contours are shown marking zero in the real and imaginary parts, as well as changes of π in the phase image. Comparison of these images with those in Fig. 6 shows that the beam has been distorted by propagating through the woven composite, not simply attenuated uniformly.

Reconstructed beam through a stitch in a woven composite

Fig. 8 shows the reconstructed images for a beam transmitted through a woven composite at the location of a through-the-thickness stitch. Contours are indicated as in the preceding two figures. Comparing these results with those in Figs. 6 and 7, one can observe a data “dimple” near the center of the main lobe of the beam, which should correspond to effects caused by the Kevlar stitch. In addition to the localized “dimple”, there is a general distortion similar to that seen in Fig. 7, caused by the woven textile fibers.

Ultrasonic Beam Through Woven Composite

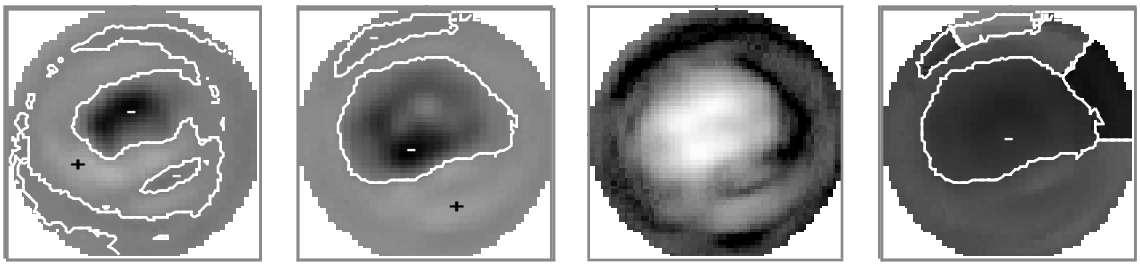

FIGURE 7. Reconstructed beam through a woven composite. Reconstructed real and imaginary parts have zero-crossing contours to indicate sign change. The log magnitude data is scaled from –42 dB to 0 dB. Unwrapped phase has contours at multiples of π.

Ultrasonic Beam Through Stitch in Composite

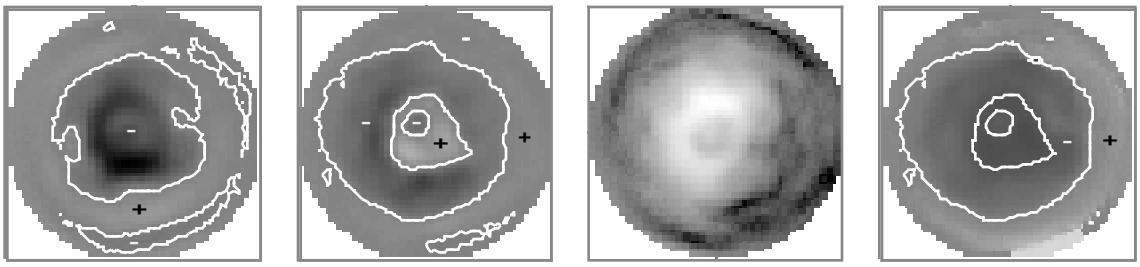

FIGURE 8. Reconstructed beam through a stitch in a woven composite. Reconstructed real and imaginary parts have zero-crossing contours to indicate sign change. The log magnitude data is scaled from –42 dB to 0 dB. Unwrapped phase has contours at multiples of π.

DISCUSSION

Modern aerospace materials and emerging experimental materials possess higher spatial variability in their elastic properties. Because these variations occur on a spatial scale similar to the wavelengths used for ultrasonic NDE, the interaction between an interrogating ultrasonic beam and these material inhomogeneities produces distortions in the beam. In a conventional ultrasonic inspection, the diameter of the receiving aperture might typically be just less than the areas reconstructed above. These receiving apertures phase-sensitively integrate the real and imaginary parts of the field over their areas, and the beam distortions, such as those displayed in Figs. 8-9, are lost.

Consider the log magnitude results from Figs. 6-8, plotted again in Fig. 9 with the grayscale compressed to highlight only the largest 15 dB of the beam, which is concentrated in the main sound beam where 70-80% of the energy is found. There is an apparent structure to the distortion caused by the woven textile fibers, in the center image. In the right-hand image, one can interpret the beam as having a similar distortion as in the center image, rotated slightly counter-clockwise, with an additional localized loss caused by the stitch. In a conventional ultrasonic inspection, these three images would be reduced to three values of a single parameter, representing the three integrated amplitudes. It clearly

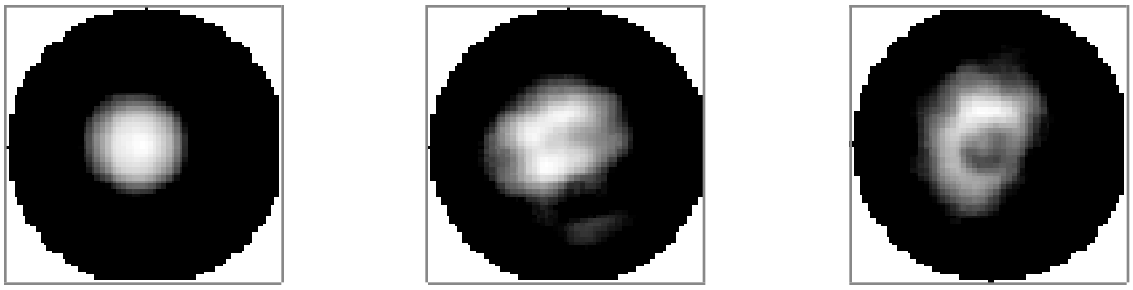

FIGURE 9. Comparison of the reconstructed log magnitude images for beams propagated through water (left), woven composite (center) and a through-thickness stitch in a woven composite (right). The grayscale has been compressed to show only the largest 15 dB of the beams, which is located in the main lobe of each beam.

takes more than one parameter to characterize the actual differences among these three ultrasonic beams, and this additional information may be valuable for the quantitative characterization of the composite.

In this paper, a novel method has been introduced which enables the high-resolution imaging of a compact ultrasonic field, such as a transmitted beam. This method provides a means to characterize the spatial information carried by the beam after passing through a complex material, such as a stitched, woven composite.

ACKNOWLEDGMENT

This work was supported in part by a NASA Graduate Student Research Fellowship NGT1-52197. The authors thank Dr. Michael Johnson of Lawrence Livermore National Laboratory for the use of his code for unwrapping of the two-dimensional phase. We thank Jeffrey Boghosian for technical assistance with the UPATS data acquisition.

REFERENCES

1. Dow, M. and Dexter, H. B., "Development of Stitched, Braided and Woven Composite Structures in the ACT Program and at Langley Research Center (1985 to 1997)", NASA TP-97-206234, 1997.
2. Giurgiutiu, V., Zagrai, A. and Bao, J. J., *Structural Health Monitoring* **1,** 41–61 (2002).
3. Stepanishen, P.R. and Benjamin, K. C., *Journal of the Acoustical Society of America*, **71**, 803-812 (1982).
4. MATLAB, The MathWorks, Inc., Natick MA, http://www.mathworks.com.
5. IDL, Research Systems. Inc., Boulder CO, http://www.rsinc.com.
6. Kak, A. C. and Slaney, M., *Principles of Computerized Tomographic Imaging*, IEEE Press, New York, 1988.
7. Ghiglia, D. C. and M.D. Pritt, *Two-Dimensional Phase Unwrapping: Theory, Algorithms, and Software*, Wiley, New York, 1998.